Solubility and transport of cationic and anionic patterned nanoparticles

Jiaye Su,[1] Monica Olvera de la Cruz,[2] and Hongxia Guo[1,*]

[1]*Beijing National Laboratory for Molecular Sciences, Joint Laboratory of Polymer Sciences and Materials, State Key Laboratory of Polymer Physics and Chemistry, Chinese Academy of Sciences, Beijing 100190, China*

[2]*Department of Materials Science and Engineering, Northwestern University, Evanston, Illinois, USA*

(Received 27 July 2011; revised manuscript received 5 January 2012; published 30 January 2012)

We analyze bulk diffusion and transport through hydrophobic nanochannels of nanoparticles (NPs) with different hydrophobic-hydrophilic patterns achieved by coating a fraction of the NP sites with positive or negative charges via explicit solvent molecular dynamics simulations. Ten different charge pattern types including Janus charged-hydrophobic NPs are studied. The cationic NPs are more affected by the patterns and have higher diffusion constants and fluxes than their anionic NPs counterparts. The NP-water interaction dependence on surface pattern and field strength explains these observations. The NP-water Coulomb interaction of anionic NPs in the bulk, which are much stronger than the hydrophobic NP-water interactions, are stronger for NPs with higher localized charge, and stronger than in the cationic NPs counterparts. The diffusion and transport of anionic NPs such as proteins and protein charge ladders with the same total charge but different surface charge patterns are slowest for the highest localized charge pattern, which also adsorb strongest onto surfaces. Our model demonstrates the separation (by reverse osmosis, capillary electrophoresis, or chromatography) of cationic NPs, including proteins with equal net charge but different surface charge distributions.

DOI: 10.1103/PhysRevE.85.011504 PACS number(s): 82.45.Yz, 47.61.−k, 66.30.Pa, 66.70.Lm

I. INTRODUCTION

Nanoparticles' (NPs) diffusion and transport properties have attracted much attention for their numerous potential applications [1–4]. For desalination [1], drug delivery [2,3], biomedicine, or biomaterials [4] applications it is essential to consider how charged particles transport across nanochannels. For example, the size and composition of NPs [2] dictate their efficiency for delivering biomolecules and drugs into cells [4,5], as well as their toxicity [5]. Moreover, their transport properties also reveal important information on the flux of organic matter including proteins and viruses through nanopores during reverse osmosis in water purification processes [6], and provides the basic knowledge to develop new NP characterization and separation techniques. Thus from the environmental, health, and technological perspectives it has become increasingly important to explore the factors that dominate the solubility, diffusion, and transport of NPs with various surface properties through nanochannels in aqueous media.

II. MOLECULAR DYNAMICS SIMULATIONS

Though the transport of water molecules through nanopores has been extensively studied [7,8], the transport of NPs as a function of their surface properties has not been analyzed. To explore new NP applications, for example, in nanofluidics [9] and biotechnology [5], and to understand their separation by reverse osmosis [1], we analyze here the diffusion and transport of NPs through nanopores as a function of their surface properties and solubility in aqueous media by molecular dynamics (MD) simulations including explicitly the water molecules. In this way, as in previous studies [10,11], we do not have to use renormalized interaction potentials (as adopted in implicit solvent NPs solubility studies [12]) and/or to use image charge methods for continuum media [13] to account for dielectric heterogeneities. In fact, the dynamics of charged molecules or ions through regions where the dielectric constant variations are unknown (such as from bulk to a nanopore) can only be modeled using explicit solvent atomistic simulations. Motivated by the highly heterogeneous surfaces of many systems including the large folded proteins captured by reverse osmosis [1], of metallic NPs functionalized with grafted thiols with end-charged groups NPs [2], of polystyrene NPs with associated proteins observed in biological fluids [3], of protein charge ladders [14], as well as of functionalized fullerene NPs with charges [15], we consider various NP types with specific charge patterns achieved by coating a fraction of the sites on the surface of individual NPs with charges [see Fig. 1(a)]. To achieve NPs water solubility, we use NPs charge densities of about $1.06e/\mathrm{nm}^2$, which is close to experimental values in large colloids [16]. In this way we can also drive them through a channel by an external electric field **E**, as shown in Fig. 1(b). For computational feasibility, we select MD simulation parameters (including tube length) following RNA translocation [17] and water transport [10,18] studies. The carbon atoms in the membranes, the channel, and the NPs hydrophobic surfaces are modeled as Lennard-Jones particles. Known carbon-carbon and carbon-water interaction parameters [7,19], the Nose-Hoover method [20] for temperature coupling and the particle-mesh Ewald method for the electrostatic interactions [21] are used. The simulations are performed with the Gromacs package and the TIP3P water model [8], and include about 6000 atoms. The MD time step is 2 fs, data are collected every 0.5 ps, and the MD runs last 210 ns.

III. RESULTS AND DISCUSSION

We first analyze the bulk diffusion of NP types ± 1 in the absence of a nanopore. Figure 2(a) indicates that the

*Author to whom correspondence should be addressed.

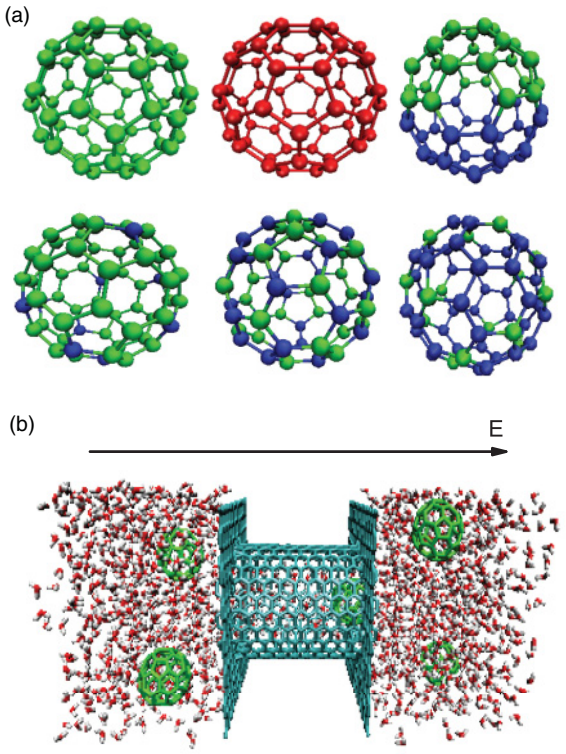

FIG. 1. (Color) (a) All NP types have $\pm 6e$ total charge, and 60 atoms (right to left, top to bottom), with charge per coated atom in parentheses: $1+ (q = +0.1e)$, $1- (q = -0.1e)$, $2+ (q = +0.2e)$, $3+ (q = +0.12e)$, $4+ (q = +0.2e)$, and $5+ (q = +0.4e)$. The anionic types $2- (q = -0.2e)$, $3- (q = -0.12e)$, $4- (q = -0.2e)$, and $5- (q = -0.4e)$; the corresponding negative NP types (not shown) have the same charge arrangement with $-$ sign. Green and red represent positive and negative charges, respectively, while blue denotes neutral. (b) A snapshot of the MD simulation system showing the hydrophobic nanometer water channel, of length $L = 2.564$ nm and diameter $D = 1.616$ nm and the two membrane sheets (turquoise green) in a periodic box with water molecules, wherein five NPs of radius $R = 0.333$ nm (bright green) are driven through it by an external electric field $\mathbf{E}$.

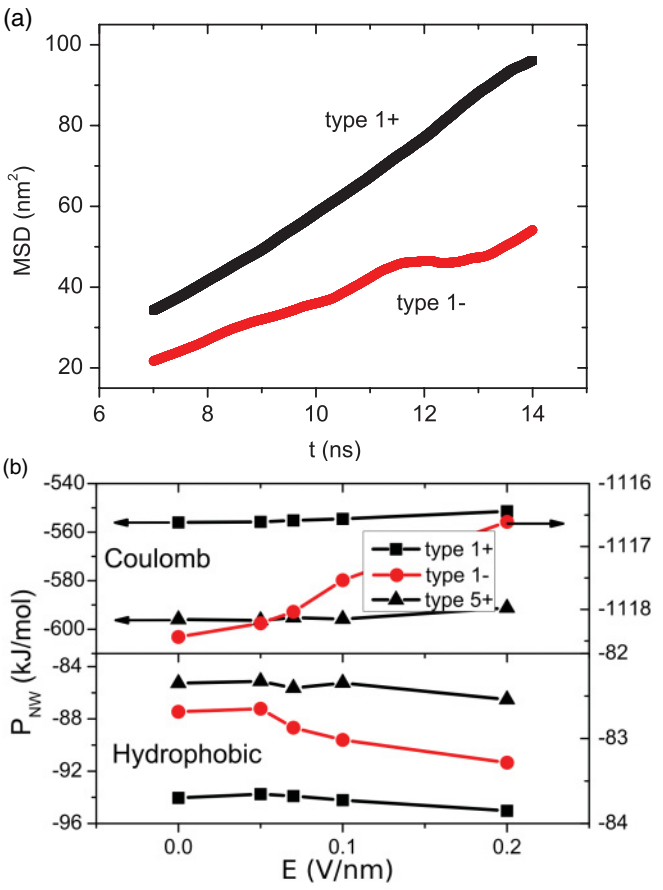

FIG. 2. (Color online) (a) The mean squared displacement of NPs for type $1+$ and type $1-$ as a function of time under $E = 0$. The resulting diffusion constants are 1.527×10^{-5} cm^2/s for type $1+$ and 0.732×10^{-5} cm^2/s for type $1-$, respectively. (b) Nanoparticle-water interactions for type $1+$ and $5+$ (left axis) and type $1-$ (right axis) as a function of the electric field. There is one nanoparticle and 1728 water molecules in each simulation, and an additional 25-ns MD run for each nanoparticle type as a function of the electric field.

diffusion constant of the cationic NPs is at least twice the one of anionic NPs. When we turn the electric field on we find converse differences in mobility (for example, at $|\mathbf{E}| = 0.05$ the mobility ratio is less than 0.9), due to the competition of electric field and self-diffusion. The differences in the diffusion constant can be attributed to the difference in nanoparticle-water interaction, P_{NW}, for cationic and anionic NPs shown in Fig. 2(b). P_{NW} is computed by the summing of the interaction energies acting on a free NP in the water. The Coulomb interactions of type $1+$ and type $1-$ are five and ten times stronger than the hydrophobic interactions, respectively, implying that the Coulomb interaction plays a dominant role in determining the self-diffusion differences. Since the Coulomb interaction of anionic NPs is roughly twice that of the cationic ones, anionic NPs favor water much more. Moreover, the water dipole orientations and density profiles near the NP surface indicate that anionic NPs have a larger capability of adsorbing water molecules than cationic ones, in good agreement with the results of NP-water potentials, which explains their lower diffusion constant. When $\mathbf{E} = 0$ we observed the same water depletion region around water-carbon interfaces reported earlier [10], which is characteristic of water-hydrophobic interfaces [11].

To understand the effect of cationic and anionic patterns on the dynamics, we designed various NPs, shown in Fig. 1(a), to symmetrically decrease the number of charged atoms to 50, 30, 15 for types $3\pm$, $4\pm$, $5\pm$, respectively, while keeping the total charge constant. In Fig. 2(b) we show that the P_{NW} of type $1+$ are considerably different than those of types $5+$. Therefore, we expect also different degrees of adsorption, as demonstrated in proteins with different charge patterns [22]. The solubility and diffusion differences are enhanced when the NPs are transferred through a nanopore. In Fig. 3(a) we show the average flux of types $1+$ and $1-$ NPs and in Fig. 3(b) the fluxes for types ± 3, ± 4, ± 5 trough a hydrophobic channel (Janus NPs types $2\pm$, fail to transport since they adhere onto the membranes). The flux is defined as the number of NPs per nanosecond exiting at one end of the channel after entering the other end. The hydration shell of the NP is distorted when it travels from bulk water into the channel since the Van der

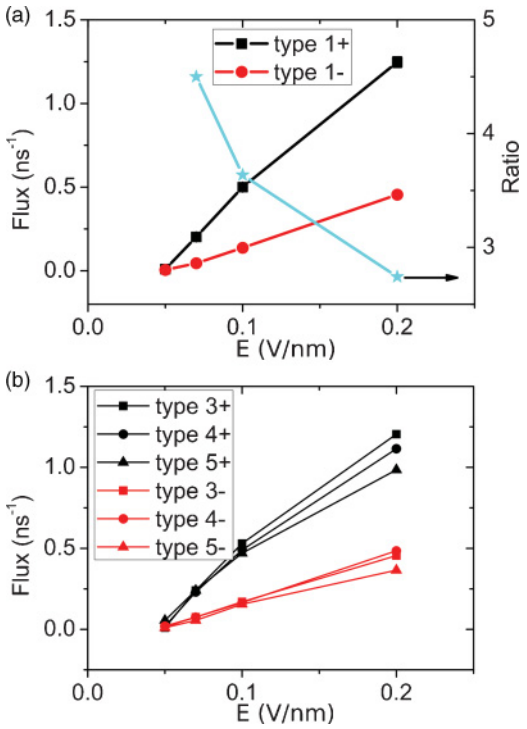

FIG. 3. (Color online) Average flux of NPs (a) for types 1± and (b) for types 3±, 4±, and 5± as a function of the electric field **E**. Note that error bars in (a) are shown for two data points and most of them are smaller than the symbols; the right axis (indicated in the plot by ⋆ symbols) is the ratio flux (1+)/flux(1−).

Waals diameter of carbon-oxygen is 0.328 nm (see Fig. 1). At $E = 0$, it is difficult to fill the channel with NPs. As E increases, the flux increases, though the values are highly dependent on the NP types, even when they are subjected to the same driving force (all ±NP types have $\pm 6.0e$ total charge). In general, the fluxes of the positively charged NPs are larger than those of the negatively charged ones. The considerably different transport of the various cationic NPs and the asymmetrical transport of cationic and anionic NPs is due to the difference in the nanoparticle-water interaction [see Fig. 2(b)]. Overall, anionic NPs with the same pattern as anionic NPs favor water and therefore overcome a higher energy barrier to enter the channel, leading to lower fluxes. The difference between the fluxes of types 1+ and 1− decreases as the field strength increases [for example, flux (1+)/flux(1−) decreases from about 4.5 to 2.7 from $E = 0.07$ to 0.2 V/nm]. The competition of the nanoparticle-water interaction (PNW) with the external driving forces is responsible for this result. At low fields, PNW dominates and this may prevent transport, which generates the maximum difference in fluxes. As the field strength increases, it becomes easier to break the hydration shell and enhance the NP flux since the force Eq dominates. Thus the difference in fluxes reduces. Interestingly, some recent experiments revealed certain differences between cationic and anionic NPs; for example, cationic NPs are more cytotoxic and more likely to induce haemolysis and platelet aggregation than anionic NPs [5].

The flux trends of types 3±, 4±, 5± are very similar to types 1±. That is, cationic types flow faster than the corresponding anionic types. In fact, as the number of charged atoms decreases, the NPs become more hydrophobic, and since the solubility of cationic NPs is inferior to their anionic counterparts, their adsorption to the membranes will also increase. Thus the flux of cationic NPs decreases relatively significantly with the decrease of charged atoms compared with the anionic counterpart as E increases. Overall, cationic NP-water interactions are weaker than anionic and therefore experience less friction. These results demonstrate that the transport dynamics of cationic NPs are more sensitive to their patterns than anionic ones.

The different results of fluxes for NPs with different charge patterns indicate that the separation and characterization of NPs should be possible via capillary and/or gel electrophoresis [23], similar to DNA analysis [24]. Though the simulation parameters were chosen to have accessible computer times to analyze the dynamics of various NP-type patterns, the observed trends should persist in experimentally accessible parameters by considering longer and wider nanopores, and the local lattice distortions due to the addition of polar groups to fullerenes [15], which are ignored here. The water-NP interaction potentials around the NPs show that anionic NPs favor water more than cationic NPs, which should persist in experimental settings. This favoring partially explains our transport results and is relevant to experimental bionano interaction observations [5], and should be useful in protein charge ladders experiments in combination with capillary electrophoresis [25].

Coulomb interactions play a dominant role in the NP dynamics. In our study the counter ions are neglected for simplicity because the charge density of individual NPs is low. One can estimate the degree of ion condensations around an NP by computing its total internal Coulomb energy $E_{\rm el}$ scaled by the thermal energy K_BT, $E_{\rm el}/(K_BT) = \int V_{\rm el}\, d^3r/(K_BT) \approx l_B^m (Z_{\rm ef})^2/R$, where R is the NPs radius, $Z_{\rm ef} = z_{\rm ef} M$ with $z_{\rm ef}$ the average effective valence of the charged unit, M is the number of charged units per NP, $V_{\rm el} \propto l_B^m/r$ with $l_B^m = e^2/K_BT 4\pi\epsilon_0\epsilon_r^m$, where e is the elementary charge, ϵ_r^m is the mean permittivity at the NPs surface, and ϵ_0 is the dielectric constant of the vacuum. Though in water l_B^w is 0.7 nm, in our settings $l_B^m \approx 1.4$ nm since $\epsilon_r^m = (\epsilon_r^w + \epsilon_r^{\rm in})/2 \approx 40$ given that in water $\epsilon_r^w = 80$ and in the NP interior $\epsilon_r^{\rm in} = 1$. The energy per number of neutralizing counterions N ($N = z_{\rm ef} M = 6$), $E_{\rm el}/N \sim K_BT$, cannot overcome the counterions entropic energy, which scales as $K_BT \ln V$, where V is the available volume fraction for free counterions, and the bulk hydration energy of the ions. Therefore counterions do not bind to NPs at highly dilute NPs bulk concentrations in salt-free conditions.

Moreover, in the presence of salt at a concentration of c_s, assuming a screened Coulomb interaction given by $V_{\rm scel}(r)/(K_BT) \approx l_B^m (Z_{\rm ef})^2 \exp(-rk)/r$, where k is the inverse screening length, $k = (4\pi l_B c_s)^{1/2}$, for any system where the number of charges N per aggregate of size R scales as $N \sim (R/a)^f$, one obtains two regimes: $E_{\rm el}/(K_BTN) \sim l_B R^{f-1}(z_{\rm ef}/af)$ for $(kR) < 1$ [26] and $E_{\rm el}/(K_BTN) \sim (l/k)^{f-1}$ for $(kR) > 1$ [27]. Since excess charge can only be at the NP surface (i.e., $f = 2$), this electrostatic potential is small if the NPs surface charge density is low (interesting effects, such as charge amplification in cationic NPs and charge

reversal in anionic NPs, arise when the surface charge density increases at high NaCl salt concentrations [28]). Therefore one expects that the ions, if attached to the NPs, will be unbounded in the presence of an external field **E**.

When we include Na^+ counterions to the anionic (type $1-$) NPs and Cl^- counterions to the cationic (type $1+$) NPs in the simulations, the MD trajectory shows that indeed the ions are not strongly bounded to the NPs since ions prefer to associate with water molecules due to their strong Coulomb interactions (hydration forces). However, we find that the ions bind with water molecules to form cluster-like aggregates of NPs with ions and water molecules at the inlet of the nanochannel. This problem due to ion-induced NPs interactions, which are enhanced in confined environments even when the NPs are weakly charged [29], is encountered in water purification via osmotic flux, where organic contaminants (such as proteins) and salt concentration gradients build at the membrane surface [6], and in protein capillary electrophoresis [25]; the problem can be alleviated by controlling the surface charge [18,25], hydrophobicity [30], or by using monovalent salts with specific cation-to-anion size ratio to reduce the ion-induce NPs interactions [31] (for example, these attractions are enhanced for anionic nanoparticles immersed in standard electrolytes where cations are smaller than anions [31]). We note that the NPs fluxes driven by **E** in the carbon nanotube diameters used here, decrease when counterions are added due also to the conduction of ions in the opposite direction since hydrated ions cannot slip trough the pore in the opposite direction of the NP fluxes. This results in larger field strengths needed to drive the nanoparticle translocation in the presence of counterions, which is not symmetric (for example, at $E = 1.0$ V/nm there is no flux for type $1-$ NPs while the flux of type $1+$ NPs is 0.7/ns). Overall, we observe comparable differences and asymmetries in fluxes between cationic and anionic NPs to those reported in Fig. 3 when salt ions are included in the simulations. Our results then show that the separation and characterization technique via NP transport through nanopores is very sensitive to the NPs surface patterns and therefore to their degree of solubility.

In a previous Na^+ and Cl^- diffusion study [32], the diffusion of the anion (Cl^-) was found to be larger than that of cation (Na^+), which is converse to our NPs case. We analyze here the transport of Na^+ and Cl^- through the nanotube of $L = 2.56$ nm for two diameters. For a diameter $D = 1.21$ nm we find an almost symmetric flux and for $D = 1.35$ nm the maximum flux ratio of Cl^- over Na^+ is only 1.22 at $E = 0.5$ V/nm. Instead, we find the opposite trend in NPs where the flux ratio of cationic to anionic NPs types $1\pm$ is always above 2.0 with a maximum about 4.5. Therefore, not only the bulk diffusion behavior but also the transportation of charged NPs through hydrophobic nanochannels are different from ions, and the water molecules are more bound to small ions than to NPs.

IV. CONCLUSIONS

In summary, we show here that charge distribution and its sign have a significant impact on NP solubility and transport properties in bulk and through nanochannels. Our analysis goes beyond static solubility differences of homogeneously charged NPs [12,33,34]. It suggests differences in adsorption to interfaces [33] and in solubility (Hofmeister series [34]) between anionic and cationic patterned NPs even if they have equal size and charge. The diffusion and average fluxes of positively and negatively charged NPs are remarkably different even if their surface charge distribution is the same. Negatively charge-patterned NPs favor bulk water environments, resulting in lower diffusion constants and in fluxes that are lower and less sensitive to the surface pattern than their positively charged counterparts. Interestingly, distinguishable biological properties between cationic and anionic NPs have been recognized experimentally [5]. This work enhances our understanding of the solubility, diffusion and transport through nanopores of NPs with patterned surfaces that exhibit charged groups in aqueous media.

ACKNOWLEDGMENTS

This work was supported by the Chinese Academy of Sciences (KJCX2-YW-H19), NSF China (20874110), the US DoD NSSEFF program (AFOSR FA9550-10-1-0167) and the NERC EFRC (DOE DE-SC0000989). We thank the Supercomputer Center of the Chinese Academy of Sciences.

[1] M. A. Shannon *et al.*, Nature (London) **452**, 301 (2008).
[2] A. Verma *et al.*, Nature Mater. **7**, 588 (2008).
[3] M. Lundqvist *et al.*, Proc. Natl. Acad. Sci. USA **105**, 14265 (2008).
[4] S. Mitragotri and J. Lahann, Nature Mater. **8**, 15 (2008).
[5] A. E. Nel *et al.*, Nature Mater. **8**, 543 (2009); C. M. Goodman *et al.*, Bioconjugate Chem. **15**, 897 (2004).
[6] E. M. Vrijenhoek, S. Hong, and M. Elimelech, J. Membr. Sci. **188**, 115 (2001).
[7] G. Hummer, J. C. Rasaiah, and J. P. Noworyta, Nature (London) **414**, 188 (2001).
[8] M. Majumder *et al.*, Nature (London) **438**, 44 (2005); J. K. Holt *et al.*, Science **312**, 1034 (2006); J. Y. Su and H. X. Guo, ACS Nano **5**, 351 (2011); S. Joseph and N. R. Aluru, Phys. Rev. Lett. **101**, 064502 (2008).
[9] A. H. J. Yang *et al.*, Nature (London) **457**, 71 (2009).
[10] S. Joseph and N. R. Aluru, Nano. Lett. **8**, 452 (2008).
[11] D. J. Bonthuis, S. Gekle, and R. R. Netz, Phys. Rev. Lett. **107**, 166102 (2011).
[12] D. Zhang, P. Gonzalez-Mozuleos, and M. O. de la Cruz, J. Phys. Chem. C **114**, 3754 (2010).
[13] R. Messina, J. Chem. Phys. **117**, 11062 (2002); A. Bakhshandeh, A. P. dos Santos, and Y. Levin, Phys. Rev. Lett. **107**, 107801 (2011).
[14] J. Gao, M. Mammen, and G. M. Whitesides, Science **272**, 535 (1996).
[15] J. Yinjie *et al.*, Nano Lett. **7**, 754 (2007); E. E. Fileti *et al.*, Nanotechnology **19**, 365703 (2008).
[16] Q. Chen *et al.*, Science **331**, 199 (2011).

[17] I. Yeh and G. Hummer, Proc. Natl. Acad. Sci. USA **101**, 12177 (2004).
[18] A. V. Raghunathan and N. R. Aluru, Phys. Rev. Lett. **97**, 024501 (2006).
[19] W. L. Jorgensen and C. Jenson, J. Comp. Chem. **19**, 1179 (1998).
[20] E. Lindahl, B. Hess, and D. van der Spoel, J. Mol. Model. **7**, 306 (2001).
[21] U. Essmann *et al.*, J. Chem. Phys. **103**, 8577 (1995).
[22] P. Gong and I. Szleifer, J. Colloid Interface Sci. **278**, 81 (2004).
[23] N. F. Steinmetz *et al.*, J. Am. Chem. Soc. **131**, 17093 (2009); G. F. Schneider *et al.*, *ibid.* **130**, 17384 (2008).
[24] D. C. Schwartz and M. Koval, Nature (London) **338**, 520 (1989); M. Olvera de la Cruz, D. Gersappe, and E. O. Shaffer, Phys. Rev. Lett. **64**, 2324 (1990); T. A. J. Duke and J. L. Viovy, *ibid.* **68**, 542 (1992).
[25] E. Cordova, J. Gao, and G. M. Whitesides, Anal. Chem. **69**, 1370 (1997).
[26] P. Gonzalez-Mozuelos and M. O. de la Cruz, J. Chem. Phys. **103**, 3145 (1995).
[27] F. J. Solis and M. O. de la Cruz, Eur. Phys. J. E **4**, 143 (2001).
[28] G. I. Guerrero-Garcia *et al.*, Soft Matter **6**, 2056 (2010).
[29] J. W. Zwanikken and M. O. de la Cruz, Phys. Rev. E **82**, 050401 (2010).
[30] A. Asatekin *et al.*, J. Membr. Sci. **298**, 136 (2007).
[31] G. I. Guerrero-Garcia *et al.*, J. Chem. Phys. **135**, 164705 (2011).
[32] S. Chowdhuri and A. Chandra, J. Chem. Phys. **118**, 9719 (2003).
[33] J. Zwanikken and R. van Roij, Phys. Rev. Lett. **99**, 178301 (2007); W. Kung, F. J. Solis, and M. O. de la Cruz, J. Chem. Phys. **130**, 044502 (2009).
[34] A. P. dos Santos and Y. Levin, Phys. Rev. Lett. **106**, 167801 (2011).